

Signal transducer and activator of transcription-6 (STAT6) inhibition suppresses renal cyst growth in polycystic kidney disease

Erin E. Olsan^{a,b}, Sambuddho Mukherjee^{a,b}, Beatrix Wulkersdorfer^{a,b}, Jonathan M. Shillingford^{a,b}, Adrian J. Giovannone^{a,b}, Gueorgui Todorov^b, Xuewen Song^c, York Pei^c, and Thomas Weimbs^{a,b,1}

^aDepartment of Molecular, Cellular and Developmental Biology and ^bNeuroscience Research Institute, University of California, Santa Barbara, CA 93106; and ^cDivision of Nephrology, University Health Network, University of Toronto, Toronto, ON, Canada M5G 2N2

Edited by Ira S. Mellman, Genentech, Inc., South San Francisco, CA, and approved September 22, 2011 (received for review July 21, 2011)

Autosomal-dominant (AD) polycystic kidney disease (PKD) is a leading cause of renal failure in the United States, and currently lacks available treatment options to slow disease progression. Mutations in the gene coding for polycystin-1 (PC1) underlie the majority of cases but the function of PC1 has remained poorly understood. We have previously shown that PC1 regulates the transcriptional activity of signal transducer and activator of transcription-6 (STAT6). Here we show that STAT6 is aberrantly activated in cyst-lining cells in PKD mouse models. Activation of the STAT6 pathway leads to a positive feedback loop involving auto/paracrine signaling by IL13 and the IL4/13 receptor. The presence of IL13 in cyst fluid and the overexpression of IL4/13 receptor chains suggests a mechanism of sustained STAT6 activation in cysts. Genetic inactivation of STAT6 in a PKD mouse model leads to significant inhibition of proliferation and cyst growth and preservation of renal function. We show that the active metabolite of leflunomide, a drug approved for treatment of arthritis, inhibits STAT6 in renal epithelial cells. Treatment of PKD mice with this drug leads to amelioration of the renal cystic disease similar to genetic STAT6 inactivation. These results suggest STAT6 as a promising drug target for treatment of ADPKD.

signal transduction | cytokines | preclinical

Autosomal-dominant (AD) polycystic kidney disease (PKD) is a common, life-threatening genetic disease and a major cause of renal failure in the United States (1, 2). Excessive proliferation and fluid secretion drive the growth of thousands of epithelial-lined, fluid-filled cysts in the kidney, which leads to destruction of normal renal parenchyma and decline in kidney function. No treatment is currently available to slow disease progression, and most patients eventually require dialysis or kidney transplantation for survival (3).

Of ADPKD cases, 85% result from mutations in the *PKD1* gene coding for polycystin 1 (PC1) (1), a multipass transmembrane protein of poorly understood function (4). We have previously shown that PC1 undergoes proteolytic cleavage, which releases its cytoplasmic tail from the membrane followed by nuclear translocation and regulation of the transcriptional activity of signal transducer and activator of transcription-6 (STAT6) (5) and STAT3 (6). Specifically, we found that the PC1 cytoplasmic tail associates with the transcription factors P100 and STAT6, translocates to the nucleus, and coactivates transcription. We have found increased levels of this cleavage fragment in ADPKD kidneys (6). Interestingly, in mouse models, both knockout or overexpression of PC1 can lead to cystic disease (7, 8).

Very little is known about the role of STAT6 in renal epithelial cells, and most studies to date have focused on its role in the immune system. Nevertheless, STAT6 is widely expressed in many tissues, including the kidney (5, 9, 10). STAT6 is activated by cytokine signaling, specifically IL4 or IL13 (9). In nonimmune cells, STAT6 is typically activated through the type-II IL4/13

receptor, a heterodimer of the IL4R α and IL13R α 1 chains (11, 12). In some cell types, STAT6 is known to positively regulate the expression of the IL4/13 receptor chains and the ligands, which leads to a positive feedback loop and persistent pathway activation (13, 14).

We now report that STAT6 is activated in renal cysts and is part of a positive feedback loop involving IL13 and its receptor, which suggests that cystic epithelial cells are permanently activated by auto/paracrine stimulation. Genetic inactivation of STAT6 in a PKD mouse model leads to significant inhibition of proliferation and cyst growth, and preservation of renal function. Treatment of PKD mice with a STAT6 inhibitory drug, the active metabolite of leflunomide, inhibits renal cyst growth as effectively as STAT6 knockout. These results suggest that STAT6 is a driving force of renal cyst growth in PKD. Therefore, STAT6 is a promising drug target for PKD treatment, especially because leflunomide is already available as a clinically approved drug.

Results

STAT6 Is Activated in Cyst-Lining Cells. To test whether STAT6 is aberrantly activated in polycystic kidneys, we investigated its level of tyrosine phosphorylation in two PKD mouse models. We recently described a human-orthologous mouse model, *Pkd1*^{cond/cond}; *Nestin*^{cre}, in which mosaic inactivation of the *Pkd1* gene leads to a robust renal cystic phenotype that replicates many important aspects of human ADPKD, including aberrant activation of mammalian target of rapamycin (mTOR) and STAT3 (6, 15). Phosphorylated (PY)-STAT6 is strongly elevated in kidneys from 7-wk-old *Pkd1*^{cond/cond}; *Nestin*^{cre} mice compared with unaffected *Pkd1*^{cond/cond} controls (Fig. 1A). Strong PY-STAT6 signals are seen in cyst-lining epithelial cells (Fig. 1C). Similar results were observed in a second, independent PKD mouse model in 21-d-old animals (Fig. 1B and D). The rapid-onset PKD phenotype in these *bpk* mice is because of a mutation in the bicaudal C gene (16). These results indicate that STAT6 is activated in renal cystic epithelial cells and may be a common feature independent of the genotype.

STAT6 and mTOR Activation by IL13 in the Kidney. STAT6 is expressed in normal kidneys (Fig. 1A and B) yet the absence of PY-STAT6 indicates that it is normally kept in an inactive state. To test whether STAT6 can be activated in normal renal tubule epithelial cells by IL4 and IL13, normal adult mice were acutely

Author contributions: E.E.O., S.M., B.W., J.M.S., A.J.G., and T.W. designed research; E.E.O., S.M., B.W., J.M.S., A.J.G., G.T., and X.S. performed research; E.E.O., S.M., B.W., J.M.S., A.J.G., G.T., X.S., Y.P., and T.W. analyzed data; and E.E.O. and T.W. wrote the paper.

The authors declare no conflict of interest.

This article is a PNAS Direct Submission.

¹To whom correspondence should be addressed. E-mail: weimbs@lifesci.ucsb.edu.

This article contains supporting information online at www.pnas.org/lookup/suppl/doi:10.1073/pnas.1111966108/-DCSupplemental.

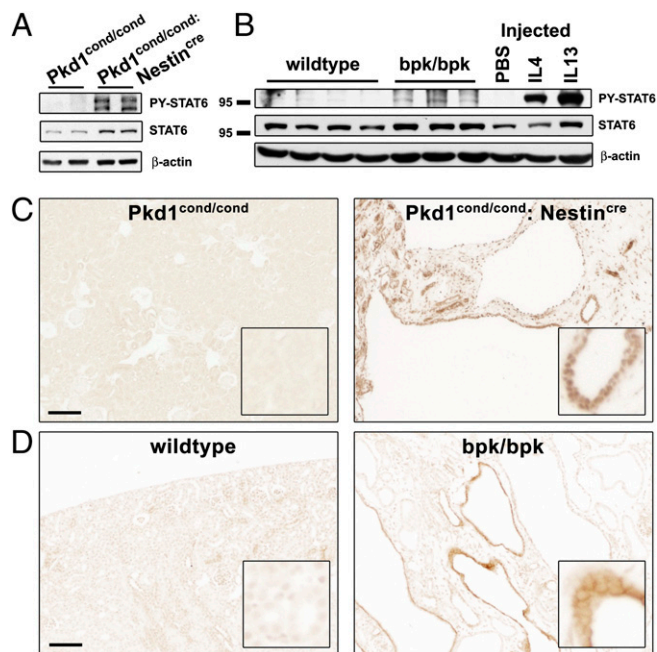


Fig. 1. STAT6 is activated in renal cysts in mouse models of PKD. (*A* and *B*) Total kidney lysates were analyzed by immunoblotting for PY-STAT6, STAT6 and β -actin. (*A*) Seven-week-old $Pkd1^{cond/cond}$ compared with cystic $Pkd1^{cond/cond}; Nestin^{cre}$ animals and (*B*) 21-d-old wild-type, compared with cystic bpk/bpk animals. For comparison, 8- to 10-wk-old wild-type animals were acutely treated for 1 h by intraperitoneal injection with cytokine (IL4 or IL13) or PBS. (*C* and *D*) Immunohistochemistry for PY-STAT6. Cyst lining renal epithelial cells in $Pkd1^{cond/cond}; Nestin^{cre}$ and bpk/bpk mice exhibit positive staining for PY-STAT6 compared with controls. (Scale bars, 100 μ m.)

challenged with these cytokines. One hour after intraperitoneal injection of either IL4 or IL13, strong PY-STAT6 signals are observed by immunoblotting (Fig. 1*B*). Immunohistochemistry revealed that STAT6 is indeed activated in renal tubule epithelial cells in addition to interstitial cells (Fig. S1). These results indicate that STAT6 can be rapidly activated in normal tubule epithelial cells in response to both IL4 and IL13, indicating that they express IL4/13 receptors and readily activatable STAT6. Tubule cells appear to respond consistently stronger to IL13 than to IL4.

In T cells, activation of the IL4R α has been shown to increase mTOR activity via IRS/PI3K (17). Because mTOR activity has been clearly linked to renal cyst growth in PKD (15, 16), we tested whether IL13 can activate mTOR in the kidney. Acute treatment of wild-type mice with IL13 indeed leads to rapid activation of the mTOR pathway, as evidenced by phosphorylation of the downstream marker S6 (Fig. S2).

Auto/Paracrine IL13 Signaling Leads to Persistent STAT6 Activation by a Positive Feedback Loop. Next, the distal tubule/collecting duct cell line Madin Darby canine kidney (MDCK) was used to investigate the mechanism of STAT6 activation in renal epithelial cells. MDCK cells normally express STAT6 but contain no detectable, activated PY-STAT6 (Fig. S3). Acute treatment with either IL4 or IL13, however, results in strong PY-STAT6 signals, suggesting that MDCK cells express IL4/13 receptors. Fully confluent, quiescent MDCK cells do not express high surface levels of the IL4R α or IL13R α 1 chains (Fig. 2*A*). Surface expression of the IL13R α 1 chain—but not the IL4R α chain—is significantly increased in actively growing, subconfluent MDCK cells. To determine if receptor chains are up-regulated because of positive feedback in renal epithelial cells, subconfluent cultures of MDCK cells were treated with IL4 for 9 h, which

resulted in strong increases in the surface expression of both the IL4R α and IL13R α 1 chains (Fig. 2*A*).

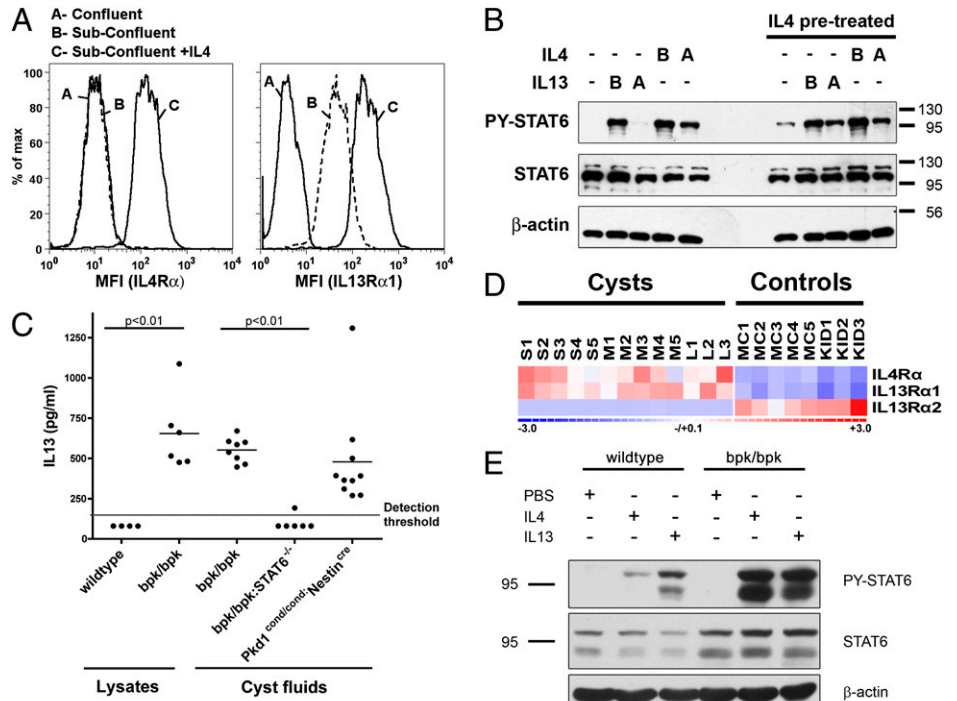
Renal tubule epithelial cells are highly polarized and may be exposed to cytokines either via their basolateral surface facing the interstitium or via their apical surface facing the tubule lumen. We investigated the relative sensitivity of fully polarized MDCK cells cultured on permeable Transwell filters toward IL4/13 from the apical and basolateral surface, respectively. Cells were acutely treated with IL4 or IL13 apically or basolaterally and the activation of STAT6 was determined by Western blot (Fig. 2*B*). IL4 was capable of activating STAT6, whether applied basolaterally or apically, although the basolateral sensitivity was more pronounced. In contrast, IL13 was only capable of activating STAT6 when applied to the basolateral side indicating that the IL13 receptor exhibits strong basolateral polarity in acutely stimulated cells.

Next, we chronically treated polarized MDCK cells with IL4 for 48 h to achieve increased surface expression of the IL4R α and IL13R α 1 chains, as shown in Fig. 2*A*. Following an unstimulated rest period, cells were then acutely restimulated with IL13 or IL4, either apically or basolaterally. As shown in Fig. 2*B*, chronic activation of the STAT6 pathway causes polarized MDCK cells to now become sensitive to apically applied IL13. This finding suggests that the IL13 receptor has either shifted its localization or increased expression in response to STAT6 activation. There is a small but consistent increase in overall STAT6 activation after IL4 pretreatment, indicating that cells have become more sensitized. Overall, these results indicate that kidney epithelial cells are capable of responding to IL4 or IL13 by phosphorylating STAT6, that they activate a positive feedback loop, and that they are sensitive to these cytokines from both apical and basolateral surfaces.

In addition to the IL4/13 receptor chains, in immune cells, the cytokines IL4 and IL13 themselves are also under positive control by STAT6, which likely contributes to the positive feedback loop by auto/paracrine activation, leading to sustained phenotypic differentiation (18). To test whether the observed activation of STAT6 in cystic epithelial cells in PKD mouse models also results in cytokine expression, we measured IL13 levels in total kidney lysates from bpk mice or age-matched wild-type controls. High levels of IL13 are present in all polycystic kidneys but undetectable in control kidneys (Fig. 2*C*). To investigate the origin of IL13 in polycystic kidneys, IL13 levels were determined in aspirated cysts fluids. Similar high levels of IL13 are present in cyst fluid from both the bpk and $Pkd1^{cond/cond}; Nestin^{cre}$ mouse models, which suggests that this represents the major pool of IL13 in polycystic kidneys. Furthermore, this suggests that cyst-lining epithelial cells are the likely source of IL13 and that they must have secreted it apically into the cyst lumen. Taken together, these results suggest that cystic epithelial cells exhibit STAT6 activation that is likely sustained by a positive feedback loop involving auto/paracrine stimulation by IL13 in cyst fluid.

To test the relevance of these findings to human ADPKD, we investigated the expression of the IL4/13 receptor chains in microdissected cysts from ADPKD patients compared with control tissue. Microarray analysis carried out as described previously (19) revealed that the gene expression of the IL4R α and IL13R α 1 chains is significantly up-regulated in cysts compared with control kidney (Fig. 2*D*), which was confirmed by quantitative RT-PCR using an expanded sample set (Fig. S4). This result is consistent with a previous gene-expression study in which the IL4R α and IL13R α 1 chains were reported to be up-regulated in kidneys of the cpk polycystic mouse model (20). We also investigated the expression of the IL13R α 2 receptor, which lacks the intracellular signaling domain and is thought to be decoy receptor and inhibitor of the STAT6 pathway (21). Strikingly, the IL13R α 2 receptor is expressed in control kidneys but is strongly down-regulated in cysts (Fig. 2*D* and Fig. S4).

Fig. 2. STAT6 activation in renal epithelial cells and autocrine/paracrine positive feedback loop. (A) Fully confluent or sub-confluent cultures of MDCK cells were analyzed for surface expression of IL4R α or IL13R α 1 by immuno-flow cytometry. Sub-confluent cells were treated with canine IL4 (4 ng/mL) for 9 h before analysis as indicated. (B) Polarized MDCK cells grown on polycarbonate filters were pretreated with or without 5 ng/mL of canine IL4 for 48 h. The media were replaced and the cells incubated for an additional 2 h in the absence of IL4. Subsequently, cells were stimulated for 30 min with or without 5 ng/mL of IL4 or IL13 from the basolateral ("B") or apical ("A") surface before analyzing cell lysates for PY-STAT6, STAT6, and β -actin. (C) Kidney lysates and pooled cyst fluids from wild-type, bpk/bpk, bpk/bpk:STAT6 $^{-/-}$, and Pkd1^{cond/cond}:Nestin^{cre} mice were analyzed for the presence of IL13 by ELISA. (D) Microarray analysis of IL4R α , IL13R α 1, and IL13R α 2 in small (S1–S5), medium (M1–M5), and large (L1–L3) cysts microdissected from human ADPKD patient samples. Minimally cystic tissue (MC1–MC5) and normal kidney (KID1–KID3) serve as controls. (E) The bpk/bpk mice are hyperresponsive to cytokine stimulation. Wild-type or bpk/bpk mice were acutely (1 h) treated with IL4 or IL13 or PBS by intraperitoneal injection, and total kidney lysates were analyzed for PY-STAT6, STAT6, and β -actin by immunoblotting.



If polycystic kidneys in mouse models exhibit increased IL4/13 receptor expression, one would expect heightened sensitivity to acute challenge with IL4/13. Indeed, acute treatment with IL4 or IL13 leads to much stronger STAT6 activation in polycystic kidneys compared with wild-type kidneys (Fig. 2E). Both cyst epithelial cells and interstitial cells exhibit this response (Fig. S5). Taken together, these results suggest that renal cysts in PKD exhibit an activated STAT6-positive feedback loop involving IL13 and the IL4/13 receptor. The inhibitory IL13R α 2 receptor may play an important role in suppressing STAT6 activity in normal kidneys.

Loss of STAT6 Leads to Decreased Cyst Growth in Vivo. Next, we investigated whether inhibition of STAT6 may affect renal cyst growth. STAT6-null mice have previously been generated and were reported to have defects in T- and B-cell differentiation but no apparent renal developmental abnormalities (22). We crossed Bpk animals with STAT6-null animals that were both in the BALB/c background. bpk/bpk:STAT6 $^{+/+}$, bpk/bpk:STAT6 $^{+/-}$, and bpk/bpk:STAT6 $^{-/-}$ offspring were obtained at the expected Mendelian ratios. Kidneys of bpk/bpk:STAT6 $^{-/-}$ animals are still grossly enlarged and polycystic compared with wild-type controls (Fig. 3A). However, the severity of the cystic disease is significantly reduced compared with bpk/bpk:STAT6 $^{+/+}$ animals, and more normal tubule tissue is apparent. Cyst diameters (Fig. 3B) and kidney weights (Fig. 3D) are significantly decreased, and the number of normal tubules is significantly increased in bpk/bpk:STAT6 $^{-/-}$ animals compared with the STAT6 $^{+/+}$ controls. Blood urea nitrogen (BUN) is strongly reduced in bpk/bpk:STAT6 $^{-/-}$ animals compared with bpk/bpk:STAT6 $^{+/+}$ animals, indicating that the lack of STAT6 leads to preservation of renal function close to wild-type animals (Fig. 3E). Bpk/bpk:STAT6 $^{-/-}$ kidneys exhibited a reduction in the number of Ki-67 positive proliferating cells (Fig. S6A), but no change in apoptotic cells (Fig. S6B), suggesting that the observed inhibition of cyst growth may be primarily because of a reduction of proliferation. Renal cyst fluid from bpk/bpk:STAT6 $^{-/-}$ animals lacked IL13 (Fig. 2C),

confirming that IL13 expression and secretion into cyst lumens is dependent on STAT6.

Renal cyst growth has previously been linked to activation of signaling pathways involving mTOR (16), extracellular signal-related kinase (ERK) (23), and STAT3 (6). Analysis of these signaling proteins using phospho-specific antibodies revealed that the lack of STAT6 does not significantly alter ERK or STAT3 activation in bpk kidneys (Fig. S6C). However, mTOR activity (as assessed by the level of P-S6) is moderately but consistently down-regulated in bpk/bpk:STAT6 $^{-/-}$ animals compared with bpk/bpk:STAT6 $^{+/+}$ animals.

Teriflunomide Treatment Alleviates the Cystic Phenotype in Vivo. These results suggested that STAT6 may be a promising drug target for the treatment of PKD. To further test this theory, we made use of the clinically approved drug leflunomide, which is used for treatment of rheumatoid arthritis. Teriflunomide, the active metabolite of leflunomide, affects several molecular targets, including dihydroorotate dehydrogenase, a key enzyme in the pyrimidine synthesis pathway, which is thought to be the mechanism underlying its efficacy in rheumatoid arthritis (24, 25). Teriflunomide also acts as a tyrosine kinase inhibitor and has been shown to inhibit STAT6 (26–28). As shown in Fig. 4A, teriflunomide inhibits the IL4-induced activation of STAT6 in MDCK cells in a dose-dependent manner. Treatment of bpk mice from postnatal days 7 to 21 with 1.4 mg/kg teriflunomide every 2 d, a clinically relevant dose, results in a very similar—or even stronger—suppression of renal cyst growth compared with genetic inactivation of the STAT6 gene (Fig. 4B). Kidney weight (Fig. 4C) and cystic index (Fig. 4D) are significantly reduced in treated animals. Renal function is largely preserved as assessed by BUN (Fig. 4E). The strong PY-STAT6 signal seen in untreated cyst-lining epithelial cells is blunted following teriflunomide treatment, indicating that teriflunomide treatment indeed leads to STAT6 inhibition in the kidney (Fig. S7A). Teriflunomide treatment does not significantly alter ERK or STAT3 activation in bpk kidneys; however, it moderately but

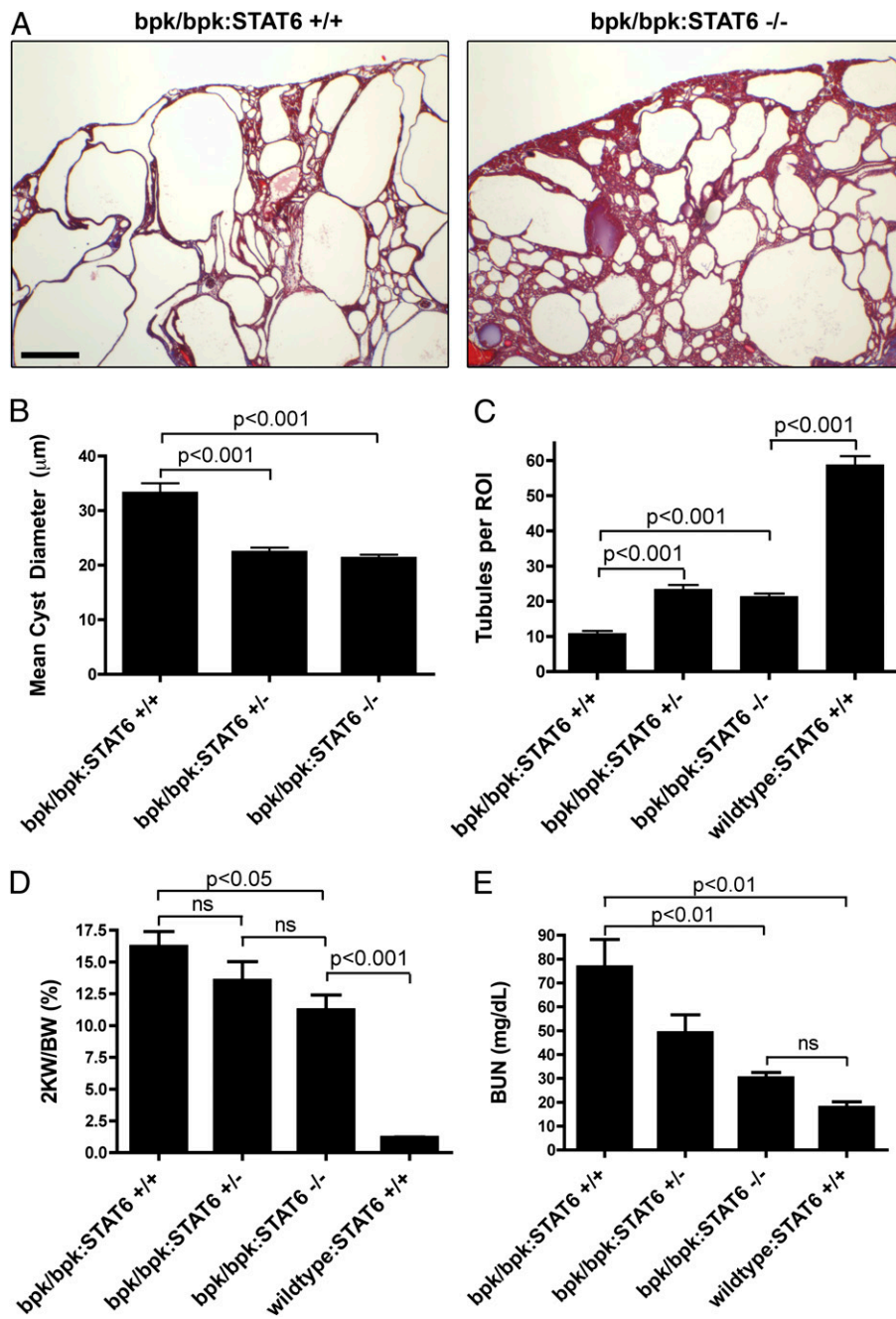


Fig. 3. STAT6 gene deletion reduces cystic disease and preserves kidney function. (A) Histology of bpk/bpk and bpk/bpk:STAT6^{-/-} kidneys. (Scale bar, 300 μm .) (B) Mean cyst diameter from morphometric analysis of H&E-stained sections. $n > 600$ cysts per genotype. (C) Tubule density from morphometric analysis of H&E-stained sections. ROI, region of interest. $n = 6$ ROI per section, $n = 4, 5, 8,$ and 4 animals per genotype, respectively. (D) Two-kidney weight to total body weight ratio (2 KW/BW) was analyzed as an indicator of cyst-growth severity. (E) Plasma BUN values were analyzed as an indicator of kidney function. $n = 12, 8, 7,$ and 6 animals per genotype, respectively.

consistently down-regulated P-S6 (Fig. S7B). We cannot exclude the possibility that other molecular targets of teriflunomide may also play a role, especially as its beneficial effect appeared to exceed that of genetic STAT6 inactivation. We observed a significant degree of toxicity of this compound in young mice, which is likely attributable to the inhibition of pyrimidine synthesis that would be expected to affect growing animals much more severely than adult animals. Future work using more specific STAT6 inhibitors appears warranted to investigate whether toxicity can be reduced or eliminated yet maintain efficacy with regard to the suppression of renal cyst growth. The observed degree of efficacy of teriflunomide treatment is in the same range as that of the mTOR inhibitor rapamycin that we previously used in the same mouse model (16).

Discussion

We have shown here that the STAT6 pathway is activated in PKD, which leads to a positive feedback loop and likely chronic auto/paracrine stimulation of cyst-lining cells via IL13 and the IL4/13 receptor. First, we have shown that renal epithelial cells in wild-type kidneys are capable of responding to acute IL13 stimulation and that STAT6 is strongly activated in two PKD mouse models (Fig. 1). Second, we have shown that MDCK cells are capable of responding to IL4/13 signaling by up-regulating their receptor chains and that these chains are up-regulated in PKD, allowing a hyperactivation of PY-STAT6 in cystic animals acutely treated with IL4/13 (Fig. 2). Finally, we have shown that STAT6 activity is at least a partial driving force of renal cyst growth because genetic STAT6 inactivation ameliorates the cystic disease (Fig. 3). Because activation of the IL4/13 receptor

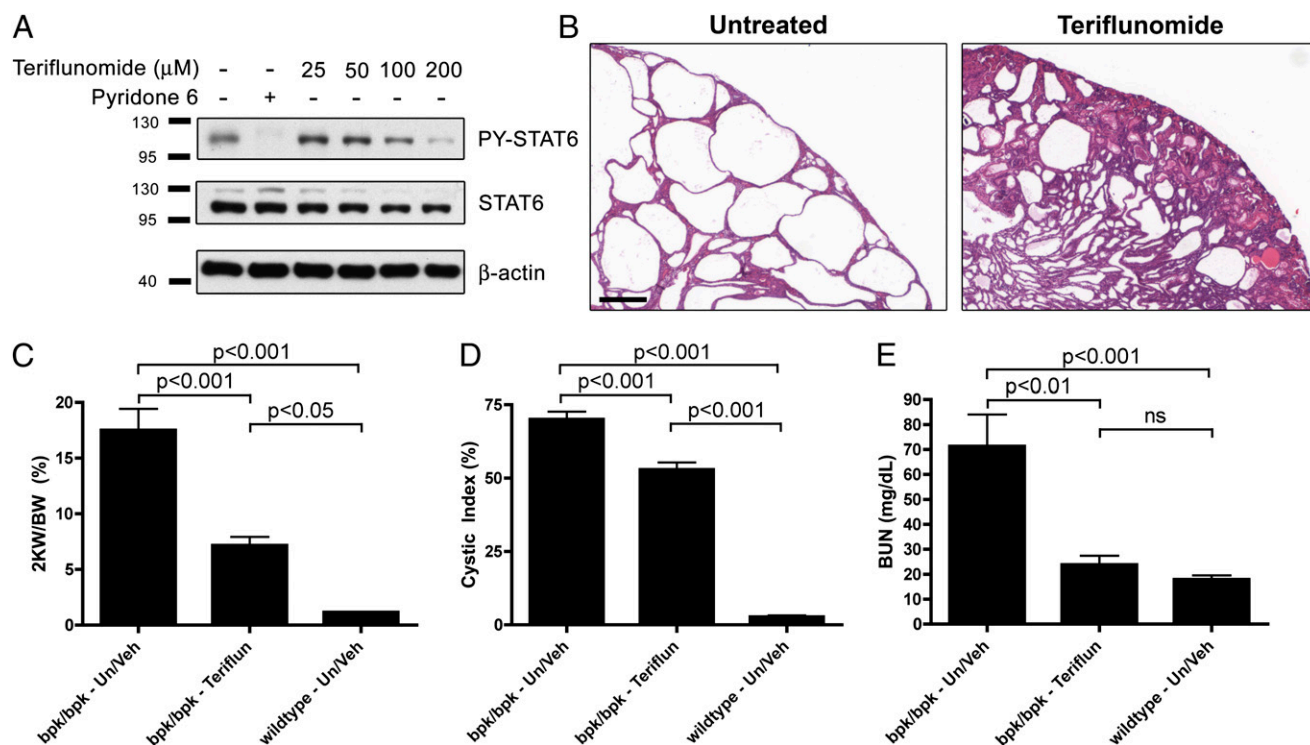


Fig. 4. The STAT6 inhibitor leflunomide/teriflunomide ameliorates renal cystic disease in bpk mice. (A) Confluent MDCK cells were treated for 2 h with the indicated doses of teriflunomide or with the pan-JAK inhibitor pyridone 6 (0.5 μM), followed by 30 min treatment with 0.1 ng/mL canine IL4 to activate STAT6 before analyzing cell lysates for PY-STAT6, STAT6, and β-actin. (B) Histology of kidneys of bpk/bpk mice treated or untreated with teriflunomide (1.4 mg/kg every 2 d) from postnatal days 7 to 21. (Scale bar, 300 μm.) (C) Two-kidney weight to total body weight ratio (2 KW/BW) was analyzed as an indicator of disease severity between bpk/bpk untreated/vehicle (Un/Veh), bpk/bpk Teriflunomide-treated (Teriflun), and wild-type untreated/vehicle (Un/Veh) mice. (D) Decrease in the degree of cystic index. (E) Plasma BUN values were analyzed as an indicator of kidney function. $n = 7, 4,$ and 9 animals per group, respectively.

also leads to mTOR activation in the kidney (Fig S2), it is possible that this mechanism could partially explain the observed aberrant activity of mTOR in ADPKD and numerous mouse models (15, 16, 29).

STAT6 plays a critical role in the adaptive immune response; it is necessary for the differentiation of T and B cells (22). In addition, IL13 and STAT6 play an important role in several human diseases, including allergic asthma, where IL13 is responsible for major characteristics of the disease, such as airway hyperresponsiveness, goblet cell hyperplasia, mucus secretion, smooth muscle hyperplasia, and subepithelial fibrosis (30). IL13 also plays a critical role in tissue fibrosis in the liver and lung (31), and in inflammatory bowel disease (32).

The role of STAT6 in the kidney is much less well understood. Because STAT6-null mice have no reported defects in renal development (22) it is unlikely that STAT6 has a critical developmental function in the kidney. We report that STAT6 is abundantly expressed in the mature kidney epithelium but does not appear to be significantly activated in normal animals (Fig. 1). Acute treatment with IL4 or IL13, however, leads to rapid STAT6 activation in normal kidneys (Fig. 2E), suggesting that it is part of a dormant pathway that can rapidly respond to a stimulus. Interestingly, overexpression of human IL13 in a rat model of renal ischemia/reperfusion injury protects from injury (33). In addition, STAT6 knock-out mice have been reported to sustain increased injury and exhibit delayed repair after renal ischemia/reperfusion injury (34). Based on these findings, we propose that the IL13/STAT6 signaling pathway plays a role in regulating tubule epithelial repair responses after renal insults. Many of the same signaling pathways and cellular processes are activated in ADPKD and in response to renal injury. This group includes pathways such as mTOR, STAT6, and STAT3, and

processes such as tubule cell proliferation, fibrosis, and deposition of extracellular matrix, and has led us to suggest that cyst growth in ADPKD represents the aberrant activation of innate renal repair programs (35). In addition, it has become clear that genetic defects in the PKD genes per se are insufficient to trigger renal cyst growth but that an additional “third hit” is required (36). Renal injury can provide such a third hit (37–40), presumably because of mitogenic signals by growth factors and cytokines (36). It is possible that the IL13/STAT6 pathway may be part of a third-hit trigger and may accelerate renal cyst growth in ADPKD patients in response to subclinical levels of renal injury.

Our results suggest that pharmacological inhibition of STAT6 may be a promising avenue for possible therapy of ADPKD. This theory is especially exciting because leflunomide is already an approved drug. Caution is warranted because leflunomide affects several molecular pathways and is a potent drug with significant side effects. Compounds that more specifically affect the STAT6 pathway (41) may prove to be superior and future research is needed to evaluate their efficacy versus side effects.

Materials and Methods

Animals. $Pkd1^{cond/cond}$, $Pkd1^{cond/cond};Nestin^{cre}$, and wt/bpk colonies were housed and fed standard laboratory chow ad libitum in a standard vivarium that was maintained at 22 to 24 °C, with a 12-h dark/light cycle. The wt/bpk animals were crossed with STAT6^{-/-} animals on BALB/c background obtained from The Jackson Laboratory. The Animal Care and Use Committee of the University of California at Santa Barbara approved all animal experiments. For cytokine stimulation experiments, 8- to 10-wk-old female C57BL/6 or postnatal day 21 bpk/bpk mice were given an intraperitoneal injection of 1 μg/100 μL of recombinant mouse IL4 or IL13 (R&D Systems). One hour after injection, the animals were killed and kidney tissue harvested. Kidneys were bisected with one-half flash-frozen in liquid nitrogen and stored at -80 °C; the other half was immersion fixed in formalin and embedded in paraffin. For

teriflunomide treatment, wt/bpk mice were bred to generate bpk/bpk animals. Pups were genotyped at postnatal day 4 and treated by intraperitoneal injection with vehicle (DMSO in 0.9% sterile saline) or 1.4 mg/kg teriflunomide (Calbiochem) every other day from postnatal day 7 to 21. Human equivalent-dose translation details are given in *SI Materials and Methods*.

Antibodies. The antibodies used in this study include [pY641]STAT6 (Santa Cruz Biotechnology), STAT6, [pY705]STAT3, STAT3, [pT202/Y204]ERK1/2, ERK1/2, [pS235/236]S6, S6, cleaved Caspase 3 (Cell Signaling Technology), IL4R α , IL13R α 1 (R&D Systems), Ki-67 (BD Pharmingen), and β -actin (Sigma-Aldrich). The E7 monoclonal antibody against β -tubulin was obtained from the Developmental Studies Hybridoma Bank, University of Iowa.

Immunohistochemistry. Four micrometer sections from formalin-fixed paraffin-embedded tissue were stained with H&E or Masson's trichrome or immunostained for PY-STAT6, PS-S6, Ki-67, or cleaved Caspase 3. Further details are given in *SI Materials and Methods*.

Flow Cytometric Analysis for Cell Surface Expression. MDCK cells from fully confluent cultures were plated at different seeding densities in MEM + 1.25% FBS for a total of 30 h. Where indicated, IL4 (R&D Systems; 4 ng/mL) was added at 21 h for the last 9 h of culture. Single cell suspensions were prepared by overnight incubation on a low-speed shaker at 4 °C with trypsin-free cell detachment solution (Mediatech) with concurrent primary or control Ab (Santa Cruz Biotech) incubation to minimize receptor internalization or cleavage. Single-cell suspensions were acquired on a Guava EasyCyte flow

cytometer and analyzed using FloJo v8 (TreeStar). Data represented as mean fluorescence intensity (MFI).

ELISA. Flash-frozen normal or cystic mouse kidney tissues were homogenized in PBS. Cyst fluids were aspirated from fresh kidneys, pooled, and flash-frozen. IL13 was quantified using a Mouse IL13 ELISA Kit (eBioscience).

Microarray and Quantitative RT-PCR. Detailed descriptions of the microarray and quantitative RT-PCR are provided in *SI Materials and Methods*. See [Table S1](#) for a list of primers used for quantitative RT-PCR.

Morphometric Analysis. H&E-stained kidney sections were used for quantitative analysis of tubule density, cyst diameter, and cystic index. Detailed descriptions provided in *SI Materials and Methods*.

BUN. Blood was collected before killing and separated using heparinized plasma collection tubes, then flash-frozen and stored at -80 °C. BUN was analyzed using the QuantiChrome Urea Assay Kit (BioAssay Systems).

Statistical Analysis. Data are expressed as means \pm SEM. Statistical analyses of one-way ANOVA with Tukey's Multiple Comparison posttests were performed using GraphPad Prism 4.0 (GraphPad Software).

ACKNOWLEDGMENTS. We thank Dawa Sherpa for technical support. This study was supported by Grants DK62338 and DK078043 from the National Institutes of Health (to T.W.) and W81XWH-07-1-0509 from the Department of Defense (to T.W.).

- Harris PC, Torres VE (2009) Polycystic kidney disease. *Annu Rev Med* 60:321–337.
- Grantham JJ (1995) The inscrutable renal cyst in ADPKD. *Nephrol Dial Transplant* 10: 1106–1109.
- Torres VE, Harris PC, Pirson Y (2007) Autosomal dominant polycystic kidney disease. *Lancet* 369:1287–1301.
- Anonymous; The International Polycystic Kidney Disease Consortium (1995) Polycystic kidney disease: The complete structure of the PKD1 gene and its protein. *Cell* 81:289–298.
- Low SH, et al. (2006) Polycystin-1, STAT6, and P100 function in a pathway that transduces ciliary mechanosensation and is activated in polycystic kidney disease. *Dev Cell* 10:57–69.
- Talbot JJ, et al. (2011) Polycystin-1 regulates STAT activity by a dual mechanism. *Proc Natl Acad Sci USA* 108:7985–7990.
- Piontek KB, et al. (2004) A functional floxed allele of Pkd1 that can be conditionally inactivated in vivo. *J Am Soc Nephrol* 15:3035–3043.
- Thivierge C, et al. (2006) Overexpression of PKD1 causes polycystic kidney disease. *Mol Cell Biol* 26:1538–1548.
- Hebenstreit D, Wirnsberger G, Horejs-Hoeck J, Duschl A (2006) Signaling mechanisms, interaction partners, and target genes of STAT6. *Cytokine Growth Factor Rev* 17:173–188.
- Hou J, et al. (1994) An interleukin-4-induced transcription factor: IL-4 Stat. *Science* 265:1701–1706.
- LaPorte SL, et al. (2008) Molecular and structural basis of cytokine receptor pleiotropy in the interleukin-4/13 system. *Cell* 132:259–272.
- Nelms K, Keegan AD, Zamorano J, Ryan JJ, Paul WE (1999) The IL-4 receptor: Signaling mechanisms and biologic functions. *Annu Rev Immunol* 17:701–738.
- Kotanides H, Reich NC (1996) Interleukin-4-induced STAT6 recognizes and activates a target site in the promoter of the interleukin-4 receptor gene. *J Biol Chem* 271: 25555–25561.
- Lee JH, et al. (2001) Interleukin-13 induces dramatically different transcriptional programs in three human airway cell types. *Am J Respir Cell Mol Biol* 25:474–485.
- Shillingford JM, Piontek KB, Germino GG, Weimbs T (2010) Rapamycin ameliorates PKD resulting from conditional inactivation of Pkd1. *J Am Soc Nephrol* 21:489–497.
- Shillingford JM, et al. (2006) The mTOR pathway is regulated by polycystin-1, and its inhibition reverses renal cystogenesis in polycystic kidney disease. *Proc Natl Acad Sci USA* 103:5466–5471.
- Stephenson LM, Park DS, Mora AL, Goenka S, Boothby M (2005) Sequence motifs in IL-4R α mediating cell-cycle progression of primary lymphocytes. *J Immunol* 175: 5178–5185.
- Lederer JA, et al. (1996) Cytokine transcriptional events during helper T cell subset differentiation. *J Exp Med* 184:397–406.
- Song X, et al. (2009) Systems biology of autosomal dominant polycystic kidney disease (ADPKD): Computational identification of gene expression pathways and integrated regulatory networks. *Hum Mol Genet* 18:2328–2343.
- Mrug M, et al. (2008) Overexpression of innate immune response genes in a model of recessive polycystic kidney disease. *Kidney Int* 73:63–76.
- Tabata Y, Khurana Hershey GK (2007) IL-13 receptor isoforms: Breaking through the complexity. *Curr Allergy Asthma Rep* 7:338–345.
- Kaplan MH, Schindler U, Smiley ST, Grusby MJ (1996) Stat6 is required for mediating responses to IL-4 and for development of Th2 cells. *Immunity* 4:313–319.
- Shibazaki S, et al. (2008) Cyst formation and activation of the extracellular regulated kinase pathway after kidney specific inactivation of Pkd1. *Hum Mol Genet* 17: 1505–1516.
- Greene S, Watanabe K, Braatz-Trulson J, Lou L (1995) Inhibition of dihydroorotate dehydrogenase by the immunosuppressive agent leflunomide. *Biochem Pharmacol* 50:861–867.
- Williamson RA, et al. (1995) Dihydroorotate dehydrogenase is a high affinity binding protein for A77 1726 and mediator of a range of biological effects of the immunomodulatory compound. *J Biol Chem* 270:22467–22472.
- Xu X, Williams JW, Bremer EG, Finnegan A, Chong AS (1995) Inhibition of protein tyrosine phosphorylation in T cells by a novel immunosuppressive agent, leflunomide. *J Biol Chem* 270:12398–12403.
- Xu X, Williams JW, Gong H, Finnegan A, Chong AS (1996) Two activities of the immunosuppressive metabolite of leflunomide, A77 1726. Inhibition of pyrimidine nucleotide synthesis and protein tyrosine phosphorylation. *Biochem Pharmacol* 52:527–534.
- Akiho H, et al. (2005) Interleukin-4- and -13-induced hypercontractility of human intestinal muscle cells—implication for motility changes in Crohn's disease. *Am J Physiol Gastrointest Liver Physiol* 288:G609–G615.
- Torres VE, et al. (2010) Prospects for mTOR inhibitor use in patients with polycystic kidney disease and hamartomatous diseases. *Clin J Am Soc Nephrol* 5:1312–1329.
- Finkelman FD, Hogan SP, Hershey GK, Rothenberg ME, Wills-Karp M (2010) Importance of cytokines in murine allergic airway disease and human asthma. *J Immunol* 184:1663–1674.
- Wynn TA (2004) Fibrotic disease and the T(H)1/T(H)2 paradigm. *Nat Rev Immunol* 4: 583–594.
- Heller F, et al. (2005) Interleukin-13 is the key effector Th2 cytokine in ulcerative colitis that affects epithelial tight junctions, apoptosis, and cell restitution. *Gastroenterology* 129:550–564.
- Sandovici M, et al. (2008) Systemic gene therapy with interleukin-13 attenuates renal ischemia-reperfusion injury. *Kidney Int* 73:1364–1373.
- Yokota N, Burne-Taney M, Racusen L, Rabb H (2003) Contrasting roles for STAT4 and STAT6 signal transduction pathways in murine renal ischemia-reperfusion injury. *Am J Physiol Renal Physiol* 285:F319–F325.
- Weimbs T (2007) Polycystic kidney disease and renal injury repair: Common pathways, fluid flow, and the function of polycystin-1. *Am J Physiol Renal Physiol* 293: F1423–F1432.
- Weimbs T (2011) Third-hit signaling in renal cyst formation. *J Am Soc Nephrol* 22: 793–795.
- Patel V, et al. (2008) Acute kidney injury and aberrant planar cell polarity induce cyst formation in mice lacking renal cilia. *Hum Mol Genet* 17:1578–1590.
- Takakura A, et al. (2009) Renal injury is a third hit promoting rapid development of adult polycystic kidney disease. *Hum Mol Genet* 18:2523–2531.
- Bastos AP, et al. (2009) Pkd1 haploinsufficiency increases renal damage and induces microcyst formation following ischemia/reperfusion. *J Am Soc Nephrol* 20:2389–2402.
- Happé H, et al. (2009) Toxic tubular injury in kidneys from Pkd1-deletion mice accelerates cystogenesis accompanied by dysregulated planar cell polarity and canonical Wnt signaling pathways. *Hum Mol Genet* 18:2532–2542.
- Oh CK, Geba GP, Molino N (2010) Investigational therapeutics targeting the IL-4/IL-13/STAT-6 pathway for the treatment of asthma. *Eur Respir Rev* 19:46–54.

Supporting Information

Olsan et al. 10.1073/pnas.1111966108

SI Materials and Methods

Human Equivalent Dose Translation. An animal dose of 1.4 mg/kg teriflunomide every other day was extrapolated to human equivalent dose of 0.114 mg/kg using body surface area conversion calculation (1). This conversion equates to a dose of 6.84 mg for a 60-kg person, which is within the 5- to 20-mg daily clinical dose range for rheumatoid arthritis patients (2, 3).

Immunohistochemistry. Four micrometer sections from formalin-fixed paraffin-embedded tissue were stained with H&E or Masson's trichrome or immuno-stained for phosphorylated (PY)-signal transducer and activator of transcription-6 (STAT6). Briefly, sections were deparaffinized in xylene, rehydrated through a series of alcohols, and then subjected to antigen retrieval by microwaving for 4 × 5 min in 10 mM sodium citrate, pH 6.0. Sections were incubated with blocking buffer (10% normal goat serum, 5% normal mouse serum, 0.5% fish skin gelatin, 1% BSA in Tris-buffered saline with 0.1% tween-20) and incubated with primary antibody or IgG control overnight. Endogenous peroxidase activity was blocked using 3% hydrogen peroxide in Tris-buffered saline and endogenous biotin was blocked using the Avidin/Biotin blocking kit (Vectastain Labs). Primary antibody was detected using the Rabbit IgG kit (Vectastain Labs) and DAB.

Microarray and Quantitative RT-PCR. U133 Plus 2.0 oligonucleotide DNA microarrays and data analysis. Renal cyst samples of varying size were obtained from five polycystic kidney disease-1 (PKD1) patients and include small cysts (SC) less than 1 mL ($n = 5$), medium cysts (MC) between 10 and 25 mL ($n = 5$), and large cysts (LC) greater than 50 mL ($n = 3$). Minimally cystic tissue (MCT) ($n = 5$) from the same patients and normal renal cortical tissue ($n = 3$) were used as controls. All tissues were dissected within 30 min of nephrectomy, snap frozen, and stored at -80°C . Total RNA was extracted from each sample using Absolutely RNA RT-PCR Miniprep Kit (Stratagene) with an on-column DNA digestion step to minimize genomic DNA contamination. Microarray samples were prepared according to the Affymetrix Two-Cycle Target Labeling Reagents for small sample (<http://www.affymetrix.com/support/>). A labeled cRNA sample was hybridized onto GeneChip Human Genome U133 Plus 2.0 Array (Affymetrix). Scanned raw data images were processed with Genechip Operating Software 1.4. Probeset signal intensities were extracted and normalized by the robust multiarray average algorithm (4), which can be found in the R package *affy* that can be downloaded from the Bioconductor project Web site (<http://www.bioconductor.org>). Significance analysis of microarrays was used to identify genes whose expression was statistically significantly different in cyst versus MCT by setting the false-discovery rate at 0.5% (5). Pathway analysis was done by using Gene Set Enrichment Analysis (GSEA)

(6). GSEA is a supervised analysis method to identify differentially expressed gene sets (groups of genes that share common biological function or coregulation) between two classes (using NOM P value < 0.01).

Validation by quantitative real-time PCR on selected genes of interest. For the quantitative PCR (qPCR) studies, we used an expanded cyst sample set: SC ($n = 16$); MC ($n = 19$); LC ($n = 3$), and MCT ($n = 16$) from the same patients and normal renal cortical tissue ($n = 4$). Total RNA was extracted using the same methods as detailed above. cDNA was generated with SuperScript II reverse transcriptase (Invitrogen). qPCR assay was performed with the ABI PRISM 7900 Sequence Detection System, using Power SYBR Green PCR Master Mix (Applied Biosystems). Primer sets for IL4R α , IL13R α 1, and IL13R α 2 were designed to the exon sequences using the Primer Express software (Applied Biosystems). A standard curve of relative concentration was calculated for each reaction run using serial dilutions of human blood genomic DNA; absolute transcript copy numbers were calculated using standard curves for each primer set (primer sequences in Table S1). The geNorm software (<http://medgen.ugent.be/~jvdesomp/genorm/>) determines the most stable housekeeping genes (7). Gene expression normalization factor based on the geometric mean of three housekeeping genes *EEF1A1*, *B2M*, and *PPIA* were calculated. The resulting calculated copy numbers were normalized against the qPCR results and are expressed as mean \pm SE. GraphPad Prism 3.0 (GraphPad Software) was used for statistical analysis of the results. Comparisons between cysts and control were done by one-way ANOVA with Tukey's multiple comparison posttest. The statistical significance was defined as $P < 0.05$.

Morphometric Analysis. H&E-stained kidney sections were used for quantitative analysis of tubule density and cyst diameter. In Adobe Photoshop CS, a blinded investigator used 80 × 80- μm regions of interest (ROI) to measure cysts and count tubules, $n = 6$ ROI per section (cortex and medulla), $n = 4, 5, 8$, and 4 animals per genotype, respectively. For cysts fully contained within or that had a portion of the cyst within the ROI, the cyst diameters were measured from epithelial to epithelial layer through the midpoint of the cyst along the longest axis of each cyst. Proliferation was determined by counting the number of cyst-lining Ki-67 positive cells as a percentage of the total number of cyst-lining cells per high-powered field, $n = 4$ fields per section, $n = 4$ animals per genotype. Apoptosis was determined by counting the total number of cleaved caspase 3-positive cells per field (kidney section), $n = 3$ animals per genotype. Cystic index was determined as described previously (8), $n = 6$ fields per section, $n = 7, 4$, and 4 animals per genotype, respectively.

1. Reagan-Shaw S, Nihal M, Ahmad N (2008) Dose translation from animal to human studies revisited. *FASEB J* 22:659–661.
2. Chan V, Charles BG, Tett SE (2005) Population pharmacokinetics and association between A77 1726 plasma concentrations and disease activity measures following administration of leflunomide to people with rheumatoid arthritis. *Br J Clin Pharmacol* 60:257–264.
3. van Roon EN, et al. (2005) Therapeutic drug monitoring of A77 1726, the active metabolite of leflunomide: Serum concentrations predict response to treatment in patients with rheumatoid arthritis. *Ann Rheum Dis* 64:569–574.
4. Irizarry RA, et al. (2003) Exploration, normalization, and summaries of high density oligonucleotide array probe level data. *Biostatistics* 4:249–264.

5. Tusher VG, Tibshirani R, Chu G (2001) Significance analysis of microarrays applied to the ionizing radiation response. *Proc Natl Acad Sci USA* 98:5116–5121.
6. Subramanian A, et al. (2005) Gene set enrichment analysis: a knowledge-based approach for interpreting genome-wide expression profiles. *Proc Natl Acad Sci USA* 102:15545–15550.
7. Vandesompele J, et al. (2002) Accurate normalization of real-time quantitative RT-PCR data by geometric averaging of multiple internal control genes. *Genome Biol* 3(7):RESEARCH0034.
8. Shillingford JM, et al. (2006) The mTOR pathway is regulated by polycystin-1, and its inhibition reverses renal cystogenesis in polycystic kidney disease. *Proc Natl Acad Sci USA* 103:5466–5471.

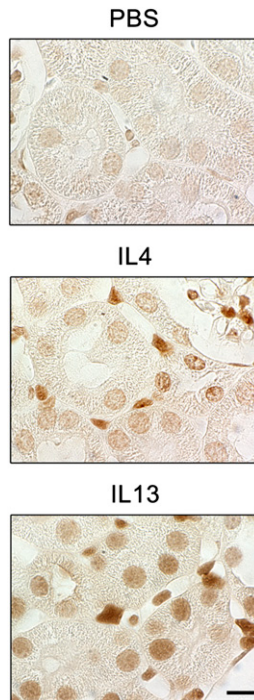


Fig. S1. PY-STAT6 is activated following acute stimulation with IL4 or IL13. Wild-type animals were injected intraperitoneally with cytokine or PBS, and kidneys harvested after 1 h. Immunostaining of renal tissue sections with PY-STAT6 reveals a prominent nuclear signal in the epithelial cells and positive staining of interstitial cells following IL13 stimulation. (Scale bar, 10 μ m.)

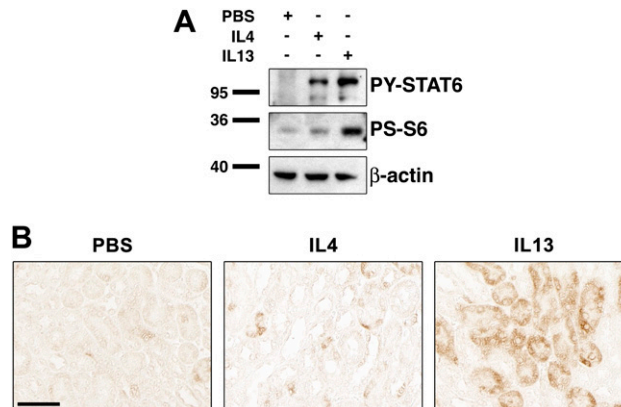


Fig. S2. Mammalian target of rapamycin (mTOR) pathway activation following injection of IL13. Immunoblot (A) and immunohistochemistry (B) for PS235/236-S6 ribosomal protein indicate that the mTOR pathway is activated in tubule epithelial cells from mouse kidney tissue after acute stimulation with IL13 for 1 h. (Scale bar, 50 μ m.)

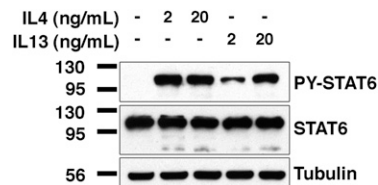


Fig. S3. Madin Darby canine kidney (MDCK) cells are capable of responding to IL4 and IL13 by phosphorylating STAT6. Subconfluent MDCK cells were treated with the indicated concentrations of recombinant canine IL4 or human IL13 for 30 min, lysed and analyzed by immunoblotting for PY-STAT6, STAT6, and tubulin.

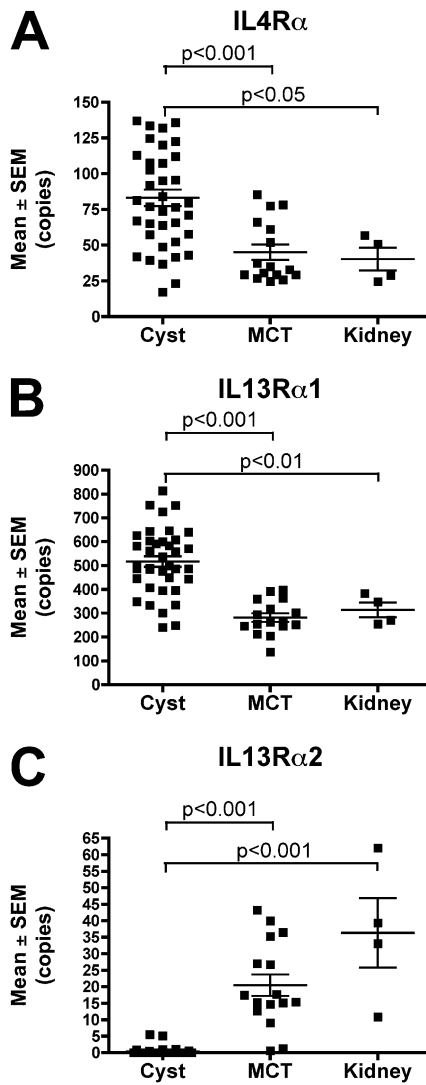


Fig. 54. qPCR validation of microarray results for IL4R α (A), IL13R α 1 (B), and IL13R α 2 (C) using an expanded sample set of microdissected cysts from autosomal-dominant polycystic kidney disease (ADPKD) patients, MCT, and normal human kidney.

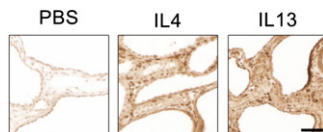


Fig. 55. Polycystic kidneys of bpk/bpk mice are hyperresponsive to activation with IL4 or IL13. Immunostaining of renal tissue sections with PY-STAT6 reveals increased signal in the epithelial cells and positive staining of interstitial cells following stimulation. (Scale bar, 50 μ m.)

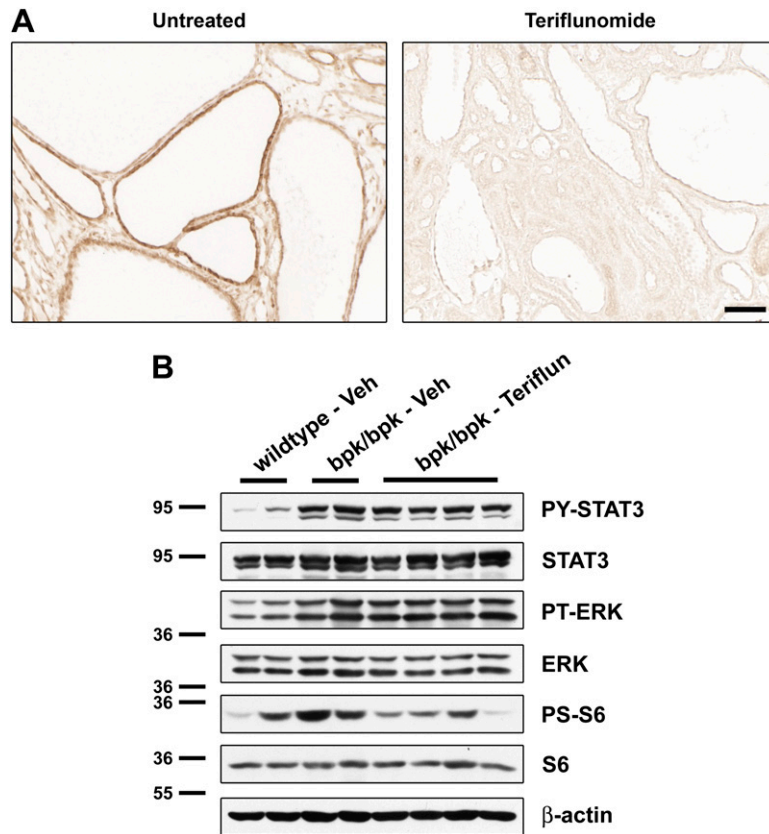


Fig. S7. Signaling pathways in leflunomide/teriflunomide-treated mice. (A) Immunostaining of renal tissue sections with PY-STAT6 reveals strong signal in untreated cyst-lining epithelial cells and little to no staining after teriflunomide treatment. (Scale bar, 50 μ m.) (B) Wild-type vehicle (Veh)-treated, bpk/bpk vehicle-treated, and bpk/bpk Teriflunomide (Teriflun)-treated kidney tissue lysates were analyzed by immunoblotting for PY-STAT3, STAT3, PT-ERK, ERK, PS-S6, S6, and β -actin.

Table S1. Primers used for qPCR

Gene name	Direction	Sequence (5'→3')	Amplicon size (bp)
<i>IL4Rα</i>	F	CACCTGCCTCTGTCTCACTGAA	77
	R	GGCCGCCCAAGTCATTC	
<i>IL13Rα1</i>	F	ATCTTTTGTCCCATCCTCTTCT	65
	R	TTCCTTTTCCCTCCCTTTTC	
<i>IL13Rα2</i>	F	AACAACAAATGAAACCCGACA	85
	R	CTCACTCCAAATTCGTCATC	
<i>PPIA*</i>	F	GGTCCGGCATCTTGCCAT	63
	R	GATGAAAAACTGGGAACCATTTG	
<i>B2M*</i>	F	GAGTGCTGTCTCCATGTTTGATGT	71
	R	AAGTTGCCAGCCCTCTAGAG	
<i>EEF1A1*</i>	F	CTGCCACCCCACTCTTAATCA	63
	R	GGCCAATTGAAACAAACAGTTCT	

Sequence are shown for forward (F) and reverse (R) primers.

*Housekeeping genes used for real-time PCR normalization.